NASA
Technical Memorandum 81398

AVRADCOM
Technical Report 79-33

SOME CONSIDERATIONS OF THE PERFORMANCE OF TWO HONEYCOMB GAS PATH SEAL MATERIAL SYSTEMS

Robert C. Bill
Propulsion Laboratory
AVRADCOM Research and Technology Laboratories
Lewis Research Center
Cleveland, Ohio

and

Lawrence T. Shiembob
Pratt & Whitney Aircraft Group
East Hartford, Connecticut

Prepared for the
Annual Meeting of the American Society of Lubrication Engineers
Anaheim, California, May 5-8, 1980

SOME CONSIDERATIONS OF THE PERFORMANCE OF TWO HONEYCOMB GAS PATH SEAL MATERIAL SYSTEMS

by Robert C. Bill
Propulsion Laboratory
AVRADCOM Research and Technology Laboratories
Lewis Research Center
Cleveland, Ohio 44135

and

Lawrence T. Shiembob
Pratt & Whitney Aircraft Group
East Hartford, Connecticut 06108

E-032

ABSTRACT

A standard Hastelloy-X honeycomb material and a pack aluminide coated honeycomb material were evaluated as to their performance as labyrinth seal materials for aircraft gas turbine engines. Consideration from published literature was given to the fluid sealing characteristics of two honeycomb materials in labyrinth seal applications, and their rub characteristics, erosion resistance, and oxidation resistance were evaluated. The increased temperature potential of the coated honeycomb material compared to the uncoated standard could be achieved without compromising the honeycomb material's rub tolerance, although there was some penalty in terms of reduced erosion resistance.

INTRODUCTION

In an aircraft gas turbine engine there is a host of seal locations. The engine schematic shown in figure 1 indicates gas path seal positions over the compressor and turbine blade tips, between rotor stages, along internal gas flow paths and adjacent to bearing cavities. All of these sealing positions are significant with respect to safe and efficient engine operation. From the standpoint of efficiency alone, reduction of clearances between compressor and turbine blade tips and the engine casing throughout a typical commercial engine by a factor of 1% of the respective blade lengths would result in a 3% to 4% improvement in engine efficiency (refs. 1 to 3). In terms of fuel consumption, 3% to 4% engine efficiency improvement is equivalent to a fuel savings of 450 000 000 gal/yr in the commercial aircraft fleet of the United States. As may be seen in figure 2, direct operating cost of an engine is extremely sensitive to fuel consumption and will become even more important as fuel costs inevitably rise.

Examples of some of the types of seal locations with which this paper will be concerned are shown in figure 3. The positions of interest include outer gas path seal positions over shrouded turbine stages and interstage seal positions between turbine stages. These positions are characterized by labyrinth knife-edge seal geometries on the rotating component with a special rub tolerant seal material on the opposing stationary component.

The primary function of the rub tolerant (or, as less accurately described, "abradable") material is to permit the maintaining of minimum clearance between the rotor and stationary component by minimizing wear to the rotor in the event of a rub interaction. The significance of minimizing rotor wear is summarized in figure 4. A typical rub occurs over a limited arc length. If the seal material is rub tolerant and wears without causing wear to the rotor, the clearance increase associated with the rub is localized, and engine efficiency penalty is minimal. If, on the other hand, the rotor wears, clearances are increased over 360° and a significant engine efficiency penalty arises.

In addition to being rub tolerant, the seal material must also resist erosion and loss of material through oxidation and corrosion. Hence, the overall requirements which a desirable gas path seal material must meet are manifold and sometimes mutually exclusive.

There are basically three broad types of rub tolerant gas path seal materials in use, summarized in figure 5, with various hybrids in experimental stages of development. First, there are the low density sintered materials; discrete particles are broken off of these materials whdn a rub occurs, and they are the seal materials most accurately described as "abradable." Second, there are the low shear strength materials including plasma sprayed Al and various organic composite systems that are essentially machined away during a rub. Third, there are the honeycomb or open structures that derive their rub tolerance from the very small solid surface involved in a rub incursion.

In this paper we will be concerned primarily with the rub behavior, erosion resistance, and other durability aspects of two different honeycomb materials intended for gas path seal applications in the turbine section of the engine. First though, let's consider how honeycomb materials actually function from the sealing standpoint in labyrinth seal configurations.

SEALING CHARACTERISTICS OF HONEYCOMB MATERIALS

The sealing effectiveness of labyrinth seals in general results from a successive series of throttlings of the sealed fluid, shown schematically in figure 6. The fluid is accelerated as it passes through the narrow passages between the knife-edge and the opposing surface. The kinetic energy increase associated with this acceleration is then dissipated in the cavities between the knife-edges. In this way, a sizable pressure drop across the labyrinth seal can be realized with a relatively small leakage or through flow. In reference 4, a convenient method of applying the well-known Egli equation to predicting labyrinth seal flow is presented and has the form: $\dot{M} = C\varphi\alpha\gamma A\,(Pu/\sqrt{Tu})$ where $\dot{M}$

is the fluid mass flow rate; φ is the flow function determined by the seal pressure ratio and the number of labyrinth stages; α is the discharge coefficient, a function of clearance and knife-edge thickness; γ is the carryover factor determined by knife-edge spacing and clearance; A is the leakage area; and Pu and Tu are the sealed fluid pressure and temperature, respectively.

Details of the overall labyrinth seal efficiency are sensitive to surface finish, porosity and geometry of the seal material opposing the knife-edges. A NASA-funded study performed at Allison (ref. 5) demonstrated some interesting phenomena associated with honeycomb seal materials, summarized in figure 7. It was discovered that in labyrinth seal configurations, the presence of the open honeycomb cavities resulted in as much as a 25% reduction in measured airflow parameter (equivalent to $C\varphi\alpha\gamma$) as compared to a solid-smooth seal. Stocker (ref. 5) attributes this significant flow reduction to the generation of turbulence in the honeycomb cells leading to more effective kinetic energy dissopation in the vavities. Perhaps another way of looking at the role of the honeycomb open cells is through a possible reduction in the carryover factor.

From the observed reduction in leakage through labyrinth seal configurations, it would appear then that over a range of clearance and geometric conditions, positive benefit in terms of engine efficiency would be expected from use of honeycomb in some seal locations.

MATERIALS

The seal materials studied in this investigation included two 1.6-mm cell size honeycomb systems. The first material which served as a baseline was a widely used Hastelloy-X (AMS-5536) hexagonal cell honeycomb system made from 0.076-mm thick alloy sheet. This material is shown in figure 8. Note the wicking of braze material between adjoining alloy sheets. Wicking is caused by capillary action drawing liquid braze material up along sharp radius corners and open spaces where Hastelloy-X sheets comprising the honeycomb are joined. Braze wicking occurred on bonding of the free-standing honey-

comb to its metal substrate, and the braze used was AMS 4778.

The second material studies was a pack aluminide coated Hastelloy-X honeycomb material, otherwise like the baseline. Free-standing honeycomb, not yet brazed to a Hastelloy-X backing, was subjected to a pack aluminide surface coating treatment. In the course of this treatment, carried out at 954° C (1750° F) for 5 hours, aluminum is transported to the Hastelloy-X surface in a chemically active halogenated state. Diffusion of aluminum into the Hastelloy-X results in an aluminum-rich surface layer about 5 μm thick. The in-situ formation of a protective Al_2O_3 layer on the aluminum-rich surface provides greatly improved oxidation resistance compared to the uncoated Hastelloy-X.

The pack aluminide coated honeycomb is also shown in figure 8. There is a significant reduction in braze wicking between the coated Hastelloy-X adjoining sheets attributed to lower surface energy of the aluminide surface. The motivation for examining the coated honeycomb was the potential increase in operating temperature afforded by the oxidation resistant coating.

In addition to the honeycomb materials reference is made, for purposes of comparison, to a 33% dense (67% porous) sintered NiCrAlY material. This material was considered as a candidate for low pressure turbine sealing applications (ref. 6), and its performance from the standpoint of rub and erosion characteristics is described more fully in reference 7.

APPARATUS AND PROCEDURE

Tests to evaluate rub tolerance and abradability of candidate gas path seal systems were performed in the dynamic abradability rig shown in figure 9. This rig consists of a rotor drive system and a seal specimen feed system.

The rotor drive system consists of an air turbine capable of driving disks up to 0.203 m (8.0 in) diameter at speeds up to 40 000 rpm. Interchangeable disks for either knife-edge or blade tip configurations are bolted to one end of a horizontal spindle shaft. A knife-edge configuration simulating low pressure turbine blade tip geometry was used for this program. The knife-edge was

5.08×10^{-4} m (0.020 in) thick, and 2.54×10^{-3} m (0.100 in) in height. The seal specimen was curved to conform to the curvature of the knife-edge rotor.

The seal specimen feed system consists of a dead-weight load carriage assembly to which the seal specimen is fastened by a suitable fixture. This carriage assembly can feed the specimen radially into the rotor at controlled rates from 2.54 to 10^{-6} m/s (0.0001 in/s) to 5.08×10^{-4} m/s (0.020 in/s). The radial motion of the specimen with respect to the rotor is defined as the incursion rate. Normal reaction force between the rotor and seal specimen is measured by a load cell installed in the carriage feed control system. For elevated temperature tests, two oxy-acetylene heaters and an electric air heater were used as shown in figure 9. One of the oxy-acetylene heaters and the electric air heater were directed at the seal specimen surface. The other oxy-acetylene heater was directed at the back of the seal specimen. The oxy-acetylene heater directed at the seal surface was turned off immediately before the rub interaction to prevent knife-edge heat damage. The second oxy-acetylene heater and electric air heater were effective in maintaining seal specimen temperature after the front heater was extinguished.

Rotor speed, seal specimen temperature at the center of the rub area, carriage travel, normal load, and torque are recorded continuously during rub interaction. Speed is sensed by a magnetic pulse counting system built into the drive turbine. Seal specimen temperature is measured with an optical pyrometer system. A linear voltage transformer system is used to measure carriage assembly travel. Knife-edge torque is measured with a Vibrac torque meter which uses a calibrated shaft, two slotted disks, and a light beam sensor which measures the twist in the calibrated shaft by the amount of light transmitted through the window opened by relative rotation of the slotted disks. These parameters were all recorded simultaneously on a multichannel high-speed lightbeam stripchart.

Wear to the rotor was determined by comparing before and after test surface profile traces (circumferential) in most cases, with some wear measurements having been made by a series of careful diametral measurements. Wear volume to the knife-edge was actually calculated by integrating the net change in circumferential profile after a wear test. Since wear was often localized to short circumferential arcs around the knife-edge periphery, wear measurements based on comparative circumferential profiles are more likely to provide an accurate wear measurement than isolated diametral measurements. Wear to the seal material was calculated on the basis of rub groove depth measurements. Rub performance of the seal materials was described in terms of a volume wear ratio (VWR) defined as the volume of rotor wear or pickup (negative wear by definition) divided by the seal wear volume. Small values for the VWR are desirable.

The erosion test rig is shown in figure 10. Erosion evaluation was carried out at gas velocities of M 0.3, with erosion gas temperatures of 1144, 1255, and 1366 K achieved through combustion of JP-4. Particulates, 80 grit Al_2O_3, were fed into the gas stream at the rate of 3 kg/hr. An erosion impingement angle of 7^o was used in all cases. Erosion results were assessed on the basis of material weight loss, translated into equivalent volume loss and on the basis of microscopic examination.

RESULTS AND DISCUSSION

Results of the rub tests for the two honeycomb materials are summarized in figures 11 and 12.

Figure 11 shows VWR and frictional torque as a function of incursion rate. The negative VMR's indicate a net transfer of seal material to the rotor. Overall, there was a clearly increased tendency for transfer of seal material to the knife-edge rotor to take place as incursion rate was increased. The frictional torque remained relatively constant over the entire range of incursion rates.

There were some points of difference in rub behavior for the two honeycomb

materials as may be seen in figure 11. The pack aluminide coated honeycomb showed a more consistent tendency to transfer to the rotor than did the standard Hastelloy-X honeycomb. It should be appreciated that transfer of seal material to the rotor is not necessarily so much better than rotor wear. Such transfer can lead to localized material buildup on the rotor through a "prow formation" mechanism (ref. 8) and cause self-machining of the seal material thereby resulting in larger clearances than would have occurred if the material behaved in an ideally rub tolerant manner (no rotor wear, no transfer). Another point of difference between the pack aluminide coated honeycomb and the standard Hastelloy-X honeycomb may be seen in the frictional torque characteristics shown in figure 11. Whereas the standard Hastelloy-X honeycomb showed an increase in friction torque as incursion rate increased from 25.4×10^{-4} to 25.4×10^{-3} mm/sec, the pack aluminide honeycomb consistently showed a torque minimum under the intermediate incursion rate conditions of 25.4×10^{-3} mm/sec.

The significance of the high rotor wear and high friction observed under the 183 m/sec rub condition (all other data on fig. 11 are for 305 m/sec rub speed) for the standard Hastelloy-X honeycomb is uncertain. The possibility exists that excessive braze wicking took place on this particular specimen promoting increased rotor wear.

Figure 12 shows the effect of seal material temperature on VWR and frictional torque. The pack aluminide coated honeycomb again showed a more consistent tendency to transfer to the rotor with perhaps increased transfer occurring at 1366 K. Temperature did not appear to have a major effect on the VWR results. Frictional torque, however, was significantly affected by temperatures greater than 1100 K, with temperature variation otherwise having a minor effect on friction torque. The reduced torque is very likely due to bulk softening of the Hastelloy-X alloy.

Examination of metallographic sections through the rub grooves and of

the rub surfaces indicates how the honeycomb materials accommodate a rub interaction. Figure 13 shows a microsection through a rubbed node between adjoining Hastelloy-X sheets of the standard honeycomb material. Salient features include displacement of a substantial volume of the rubbed material through a mechanism of plastic deformation. Near the rub surface there is evidence of extremely high strain rate plastic deformation - note the lamellar honeycomb wear morphology. Also note the adhereing braze alloy, intact on the rub surface. The braze material is hard and birttle, potentially abrasive to the opposing knife-edge.

Figure 14 shows a section and plan view of a rubbed note on a pack aluminide coated honeycomb specimen. The pack aluminide coating, 5 to 10 μm thick, may be seen on the external faces of the adjoining Hastelloy-X sheets - presumably the coating is present but much thinner on the interior faces. The rub forces resulted in separation of the adjoining sheets comprising the honeycomb node. There is no evidence of braze wicking in the node, but there is evidence of some crack propagation about 1/3 of the way through the alloy sheet, starting at the alloy/coating interface. In comparing figure 13, it is seen that very little plastic deformation accompanied the rub of the pack aluminide coated honeycomb. Figure 14 combined with the VWR measurements suggest that material cleanly fractured from the coated honeycomb, aided by preexisting cracks, and adhered to the opposite knife-edge forming a small abrasive cutting tool. The furrowed appearance of the rub surface itself is consistent with features seen on abraded surfaces for copper (ref. 9).

Examination of the Waspalloy knife-edge rotor, shown in figure 15, indicates that the contact was very nonuniform during rub interactions. Heat discoloration scallops are located periodically around the knife-edge periphery, and profile traces indicate these scallops to be regions of localized wear. These features were typical of rub tests against honeycomb materials as well as some sintered materials (refs. 6 and 10).

To further study these localized high temperature contact phenomena, high frequency response pyrometry instrumentation was applied to one rub interaction test involving the standard Hastelloy-X honeycomb seal material. Two pyrometers were employed, both focused on the rotating knife-edge. One was located 20° after the exit from the contact area, the other 110° away from the contact area (90° away from the first pyrometer). Examples of the temperature traces from these pyrometers are shown in figure 16. Taking into account the rate of decay of the temperature peak as the rotor hot spot passes from the 20° to the 110° pyrometer, it is estimated that local temperature of 1350 K (2000° F) are reached over a 10° to 20° arc on the knife-edge during the rub event. Obviously this means that the contact experienced by the rotor is very nonuniform and is concentrated at one or two locations around the periphery at a given time. The mechanism giving rise to these localized contacts is believed to be that of surface thermo-elastic instabilities described by Burton (ref. 11). Briefly, the scenario is as follows: (1) by chance, a small region on the rub surface is subjected to slightly heavier rub loading than adjacent regions; (2) higher frictional heat input to this small region leads to localized thermal expansion; (3) the localized thermal expansion, in turn, leads to yet heavier local loads and heat input; (4) and so it goes until wear of the local region finally leads to relief of the concentrated contact. The combination of rubbing materials here would certainly lend itself to thermoelastic instabilities. The volume averaged conductivity of the honeycomb is about two orders of magnitude lower than that of the knife-edge. Hence, the bulk of the frictional heat would be expected to flow into the knife-edge rotor, leading to thermal distortions and instabilities in the rotor.

A comparison between the pack aluminide coated honeycomb rub performance and the rub performance of a 38% dense sintered NiCrAlY (ref. 7), is shown in figure 17. It is seen that at 1366 K some rotor wear did accompany the rub against sintered NiCrAlY at a 305 m/sec rub speed, and substan-

tial transfer of material to the rotor was seen at 183 m/sec. The rub performance of the pack aluminide honeycomb was slightly better than the sintered NiCrAlY fibermetal in terms of extremes of VWR observed. One difficulty with the sintered NiCrAlY was its tendency to smear during knife-edge rub interactions.

As a further note on the rub performance of pack aluminide coated honeycomb, one test was conducted in which a 5 mm axial sweep of the rotor was introduced after the standard 76.2×10^{-3} mm incursion. As was the case for the purely radial incursions, transfer of coated honeycomb seal material to the rotor occurred in the axial sweep tests, and some smearing and folding over of cell walls was observed. In comparison, a similar test conducted against 33% dense sintered NiCrAlY fibermetal led to rotor wear, the VWR being 0.005, and the torque level was 50 times higher than for the rub against pack aluminide coated honeycomb. No axial sweep tests were conducted on the standard Hastelloy-X honeycomb.

Hot particulate (Al_2O_3 erosion particles) erosion test results for the two honeycomb materials are summarized in figure 18, along with the results for 33% dense sintered NiCrAlY fibermetal from reference 7. Recall that the results, expressed in terms of volume removal rate, are actually based on weight loss measurement. The standard (uncoated) Hastelloy-X honeycomb material exhibited the least material removal, and the rate of erosion did not appear to be very sensitive to temperature. In comparison, the measured weight loss on the pack aluminide coated honeycomb was about five times as high as the standard Hastelloy honeycomb at 1144 K and increased rapidly with increasing temperature to 1366 K where rate of erosion was about eight times as great as the standard honeycomb. The sintered NiCrAl was intermediate between the standard honeycomb and the coated honeycomb over the entire temperature range.

The appearance of the eroded surfaces of the standard honeycomb ma-

terial and the coated honeycomb, shown in figures 19 and 20, respectively, indicate a fundamental difference in erosion mechanisms for these two materials. The cell walls of the standard Hastelloy-X honeycomb material are folded over in the direction of the erosion stream. Since little seal material was actually removed the measured weight losses were low. In terms of potential clearance losses, however, the standard honeycomb material is not so different from the pack aluminide coated honeycomb from which material comprising the walls oriented perpendicular to the erosion was actually removed. It shoul d be born in mind that these are accelerated erosion tests, and the relationship between such a rig erosion environment and the erosion environment of the engine is not well documented. Note that there was no material removed for one test conducted without Al_2O_3 particulates at 1366 K on the coated honeycomb seal material.

Finally, the honeycomb seal materials were subjected to static oxidation testing at 1366 K for 50 hours. The test results indicated, as expected, that 1366 K is substantially beyond the limits of standard Hastelloy-X honeycomb - rapid breakaway oxidation had occurred with deterioration of the Hastelloy-X sheet comprising the honeycomb. In contrast, the aluminide coating provided effective protection to the Hastelloy-X cell walls, with only superficial pitting of the aluminide coating taking place. Some oxidation of the braze material was observed, though. Thirty-three percent dense sintered NiCrAlY, subjected to the same oxidation exposure, showed complete oxidation of about 1/3 of the specimen after the 50-hour test.

CONCLUSIONS

Based on fluid dynamic considerations, rub tolerance evaluation, erosion resistance and oxidation resistance of both a standard Hastelloy-X honeycomb seal material and a pack aluminide coated honeycomb material, the following conclusions are drawn:

1. Sealing benefits in terms of reduced leakage might actually arise from

application of honeycomb materials to judiciously selected interstage labyrinth seal positions and outer gas path seal positions over shrouded turbine blade tips equipped with labyrinth seal knife-edges.

2. The rub tolerance of Hastelloy-X honeycomb seal materials was not adversely affected by application of a pack aluminide coating to the honeycomb.

3. The standard Hastelloy-X honeycomb and the pack aluminide coated honeycomb showed fundamentally different erosion characteristics and rates of material removal. In terms of clearance effects attributable to erosion, the differences were not so significant.

4. Pack aluminide coated honeycomb showed potential for higher temperature application than the standard Hastelloy-X honeycomb.

REFERENCES

1. Mahler, F. H., "Advanced Seal Technology," PWA-4372, Pratt & Whitney Aircraft, East Hartford, Conn., 1972. (AFAPL-TR-72-8, AD-739922).

2. Haas, J. E. and Kifskey, M. G., "Cold-Air Performance ofa 12.766 Centimeter-Tip-Diameter Axial-Flow Cooled Turbine. III - Effect of Rotor Tip Clearance on Overall Performance of a Solid Blade Configuration," NASA TP-1032, 1977.

3. Gray, D. E. and Dugan, J. F., "An Early Climpse of Long-Term Subsonic Commercial Turbofan Technology Requirements - Fuel Conservation," AIAA Paper 75-1207, Sep. 1975.

4. Zuk, J., "Dynamic Sealing Principles," NASA TM X-71851, 1976.

5. Stocker, H. L., Cox, D. M., and Holle, G. F., "Aerodynamic Performance of Conventional and Advanced Design Labyrinth Seals with Solid-Smooth Abradable and Honeycomb Lands," EDR-9339, Detroit Diesel Allison, Indianapolis, Ind., Nov. 1977. (NASA CR-135307).

6. Shiembob, L. T., "Continued Development of Abradable Gas Path Seals," PWA-5314, Pratt & Whitney Aircraft, East Hartford, Conn., Nov. 1975. (NASA CR-134859).

7. Bill, R. C. and Shiembob, L. T., "Friction and Wear of Sintered Fiber-metal Abradable Seal Materials," NASA TM X73650, 1977.

8. Antler, M., "Process of Metal Transfer and Wear," Wear, 7, pp. 181-203 (1964).

9. Ives, L. K., "Microstructural Changes in Copper Due to Abrasive, Dry and Lubricated Wear," Wear of Materials, 1979, American Society of Mechanical Engineers, New York (1979), Eds. Glaeser, W. A., Ludema, K. C., and Rhee, S. K., pp. 246-256.

10. Shiembob, L. T., "Development of Abradable Gas Path Seals," PWA-TM-5081, Pratt & Shitney Aircraft, East Hartford, Conn., Aug. 1974. (NASA CR-134689).

11. Kilaparti, S. R. and Burton, R. A., "Pressure Distribution for Patch-like Contact in Seals with Frictional Heating, Thermal Expansion, and Wear," J. Lubr. Technol., 98, 4, pp. 596-601 (1976).

12. Grayson, K., "Improved Maintenance Practices - The Airlines' Contribution to Lower Ownership Costs," SAE Paper 760504, May 1976.

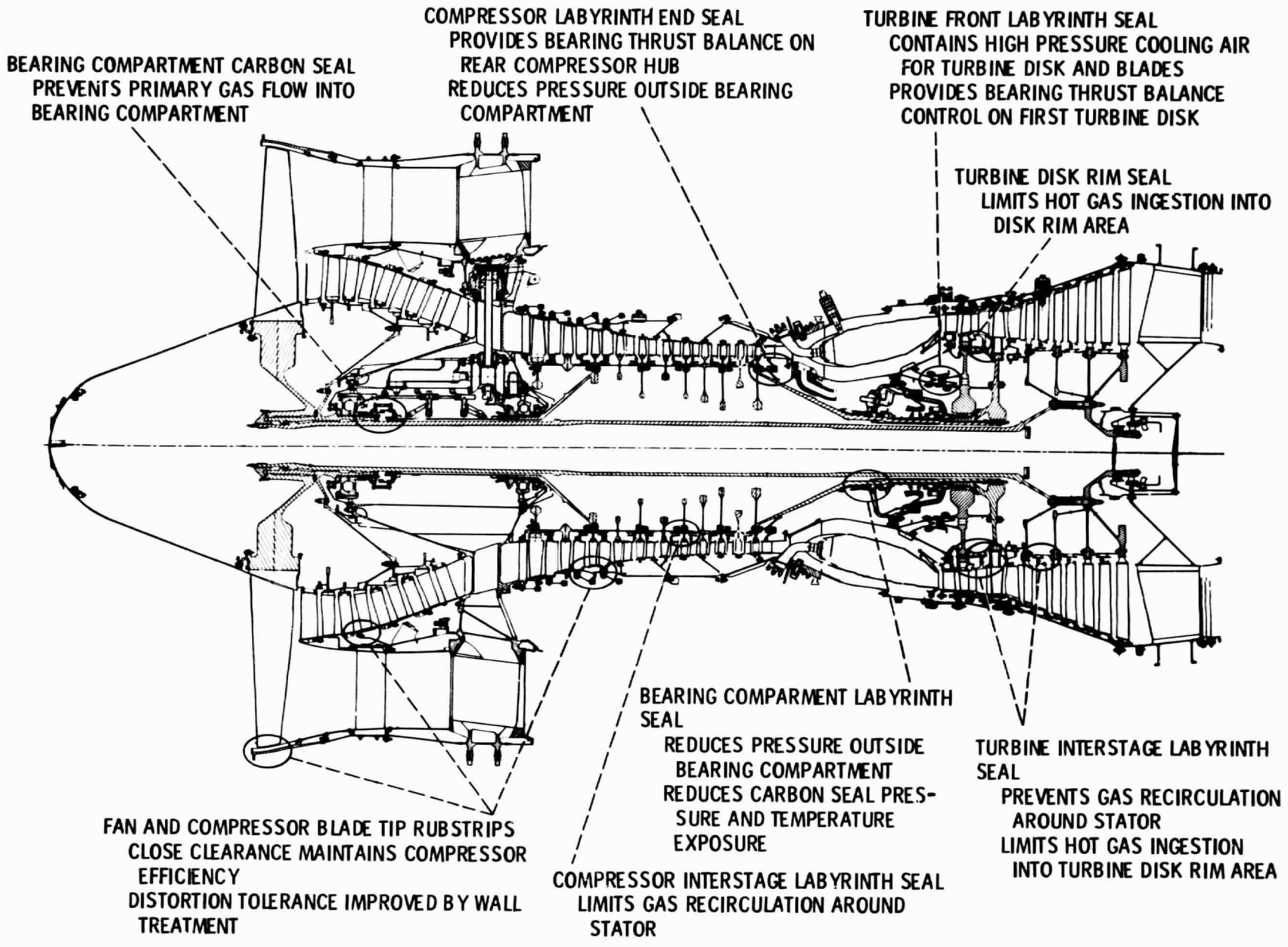

Figure 1. - Modern transport engine (from ref. 1).

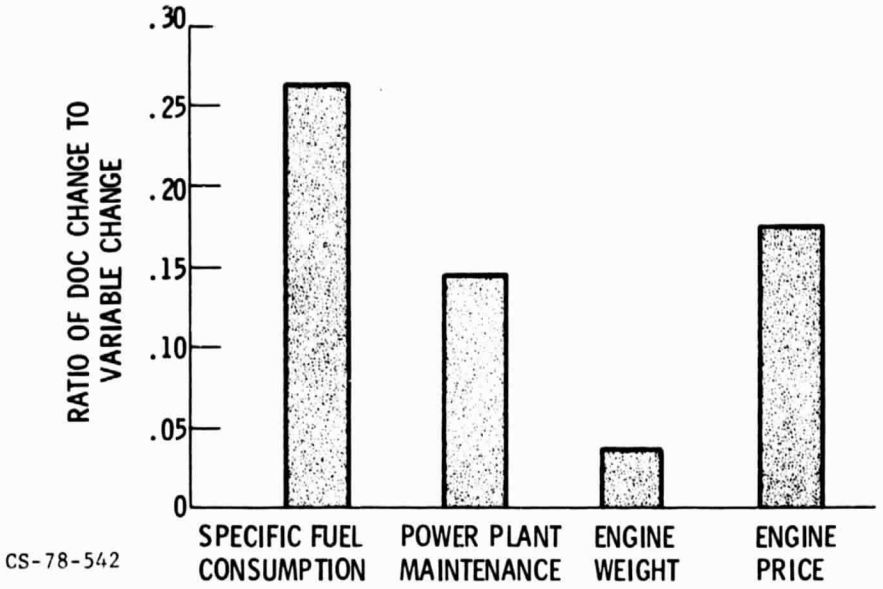

Figure 2. - Direct operating cost-sensitivity to propulsion system variable (from ref. 12).

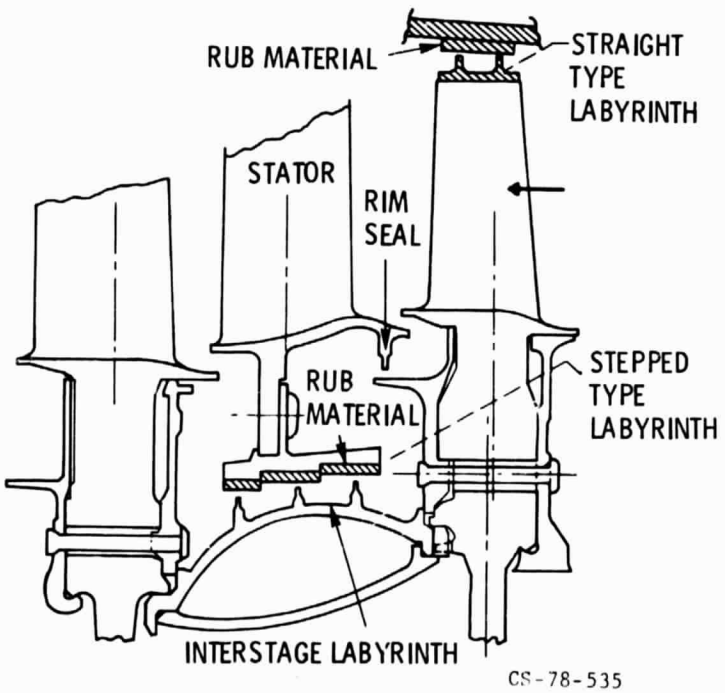

Figure 3. - Turbine sealing locations; shrouded rotor and interstage (ref. 1).

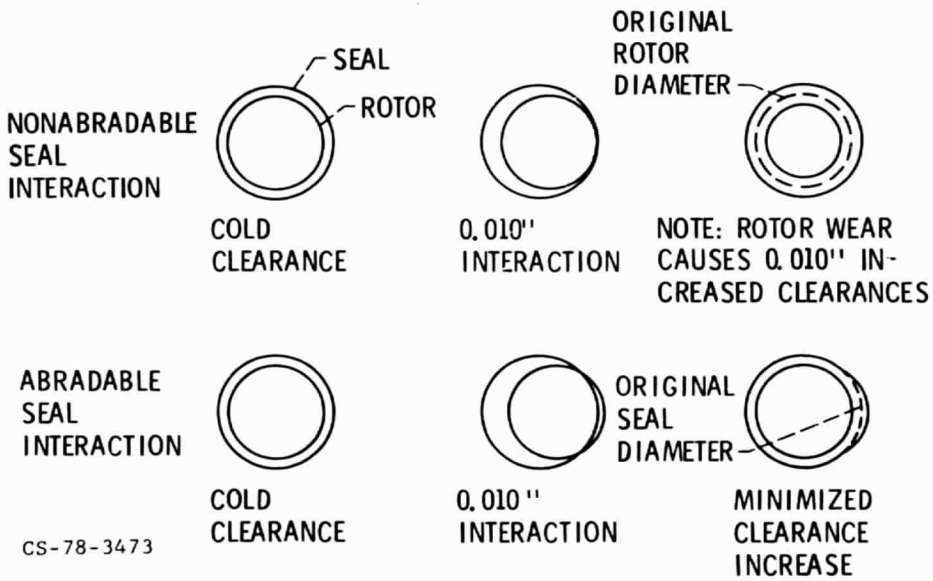

Figure 4. - Effects of rub interactions on gas path seal clearances.

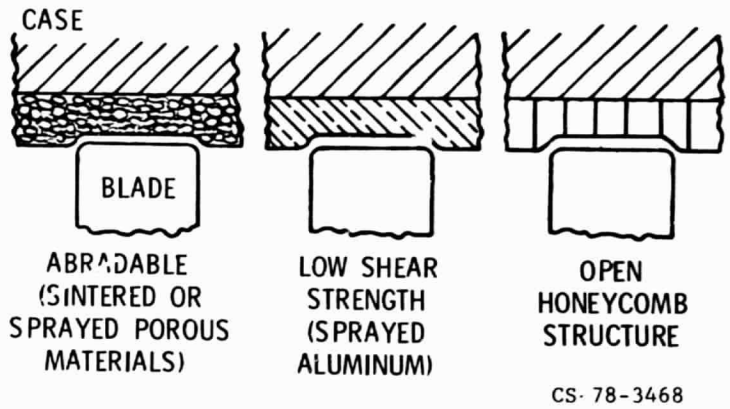

Figure 5. - Illustration of types of abradable seal materials for outer air sealing.

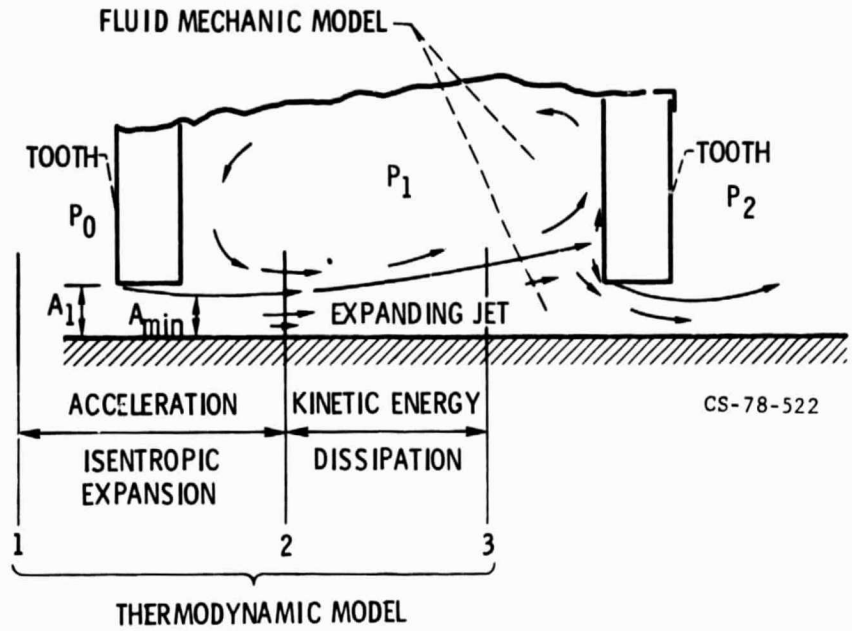

Figure 6. - Labyrinth seal, thermodynamic, and fluid mechanic models.

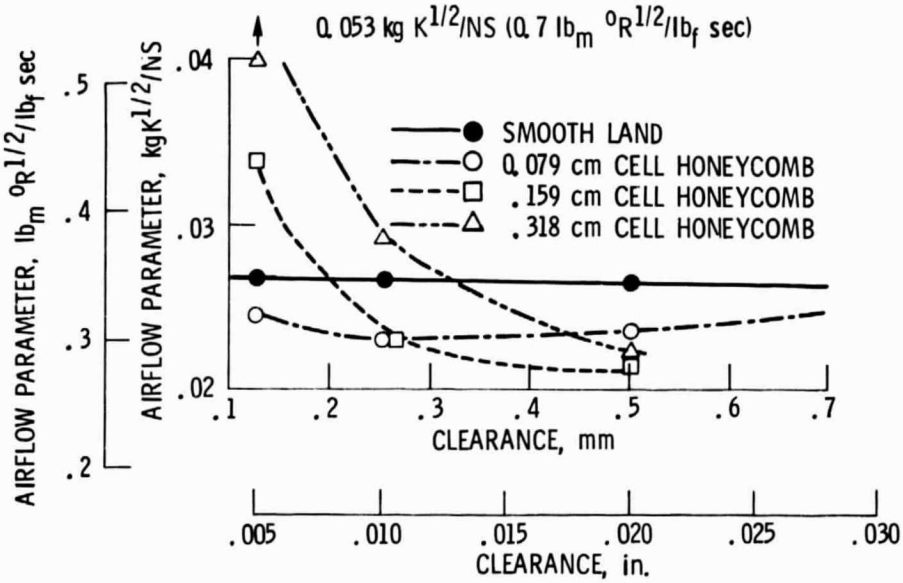

Figure 7. - Leakage characteristics of various cell size honeycomb materials as a function of clearance for a 4-tooth straight through labyrinth seal configuration (ref. 5). Pressure ratio, 2.0.

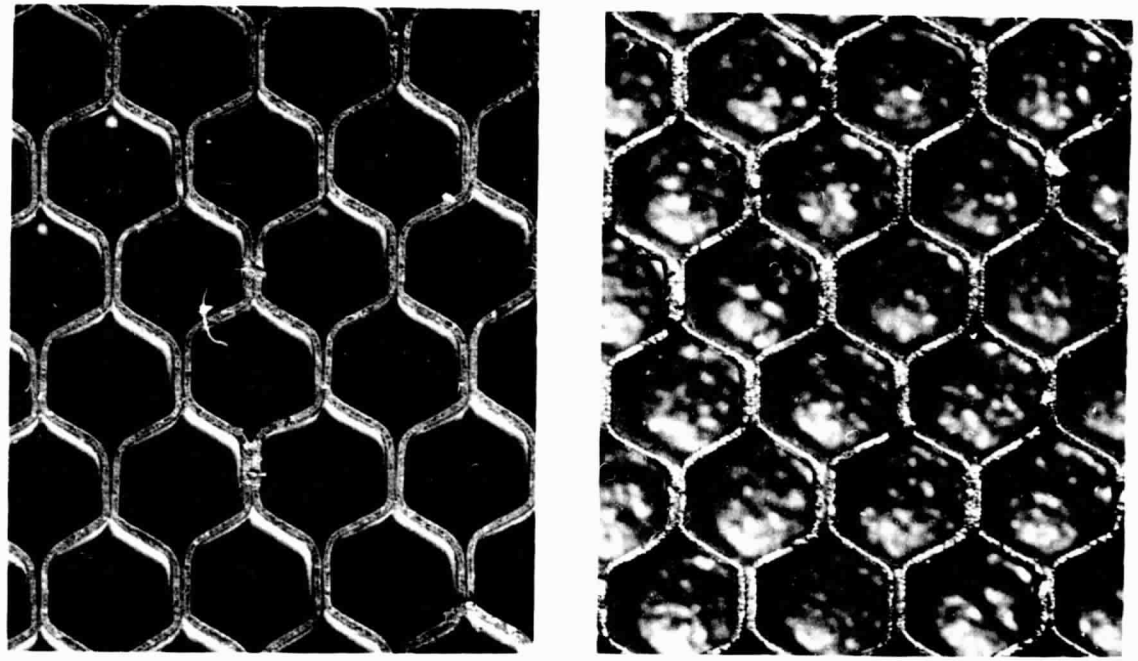

(a) PACK ALUMINIDE COATED. (b) UNCOATED HASTELLOY-X.

Figure 8. - Top view of 1.6 mm cell size Hastelloy-X honeycomb systems, showing wicking of brazing alloy between honeycomb cells.

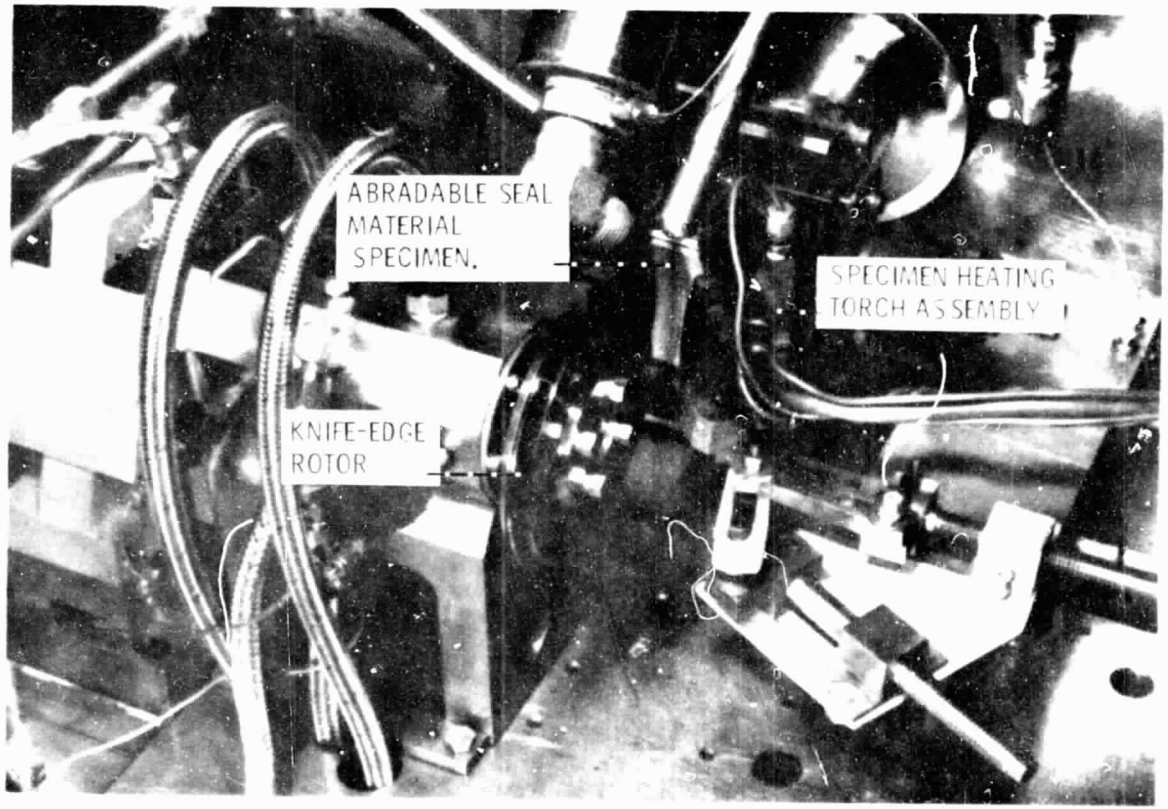

Figure 9. - Rub test apparatus.

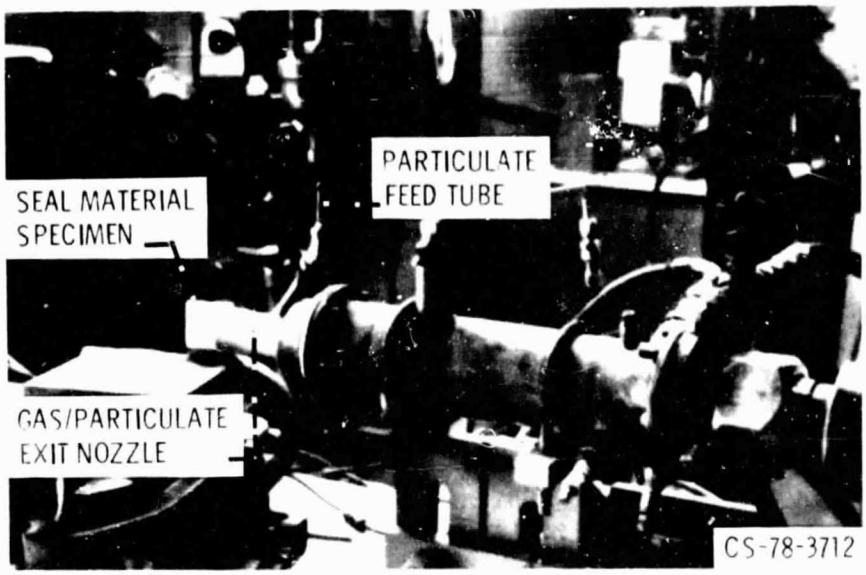

Figure 10. - Hot particulate erosion rig.

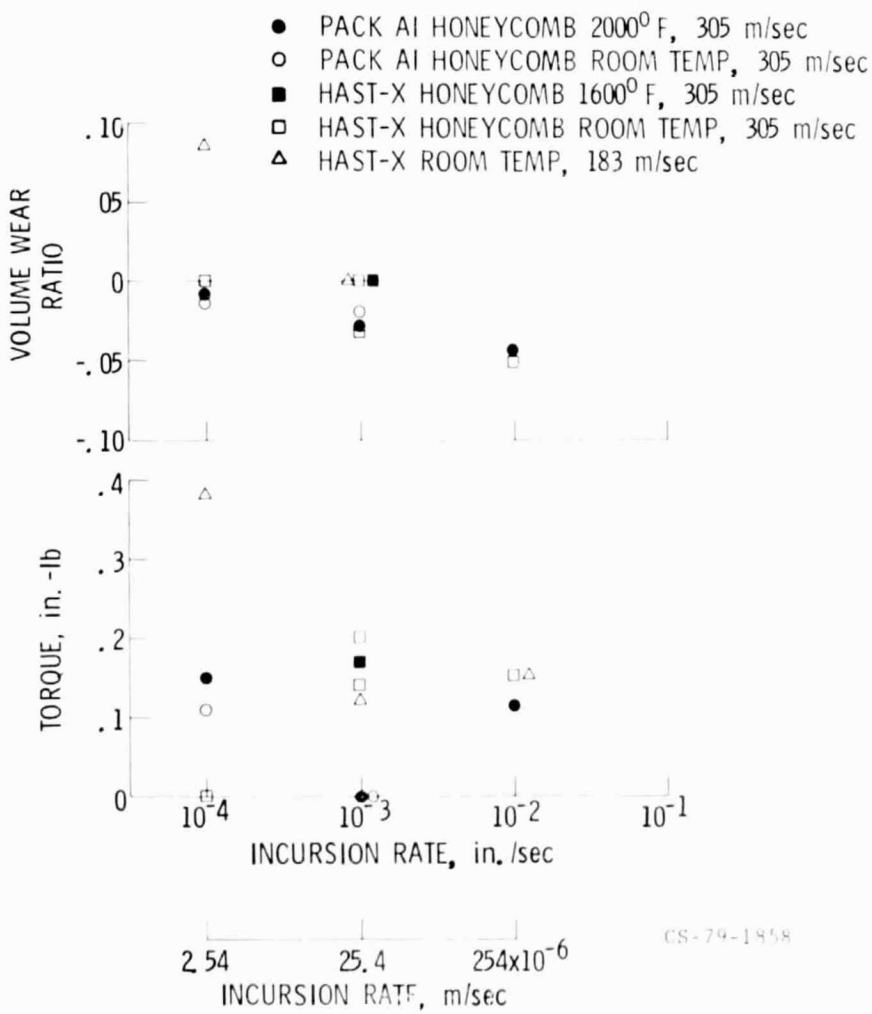

Figure 11. - Volume wear ratio and friction torque versus incursion rate for Hastelloy-X honeycomb and pack aluminide coated honeycomb.

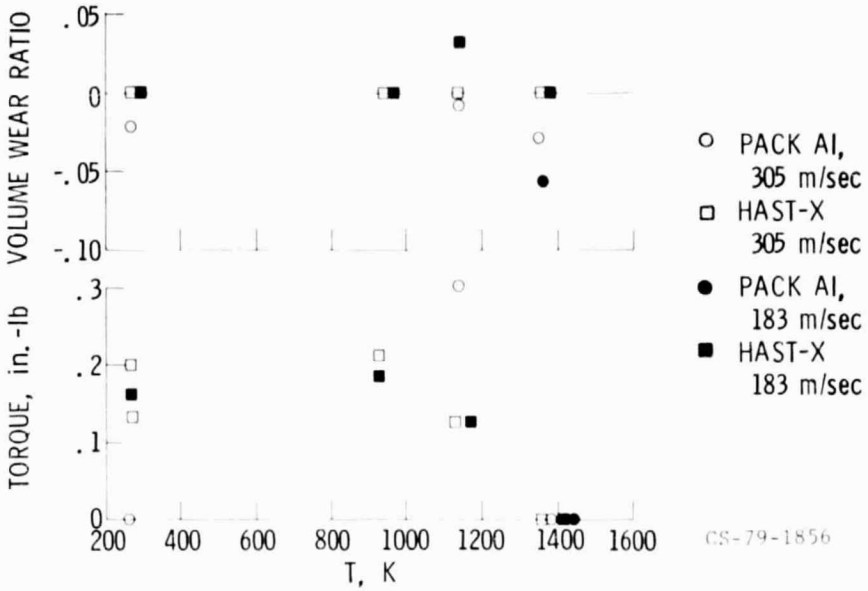

Figure 12. - Volume wear ratio and friction torque versus test temperature (25.4×10^{-6} m/sec incursion rate conditions in all cases).

(a) SECTION THROUGH NODE.

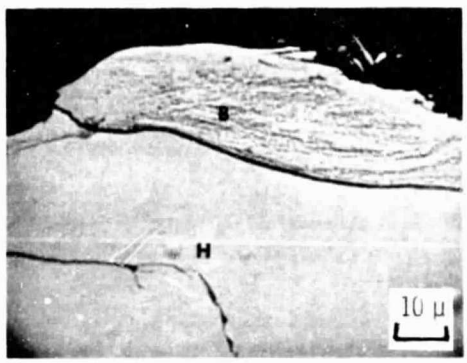

(b) HONEYCOMB MATERIAL (H) AND BRAZE ALLOY (B) ON RUB SURFACE.

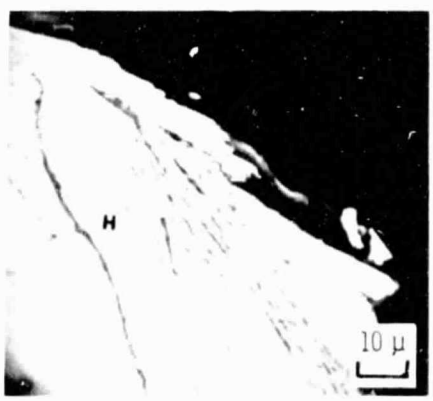

(c) HEAVILY DEFORMED HONEYCOMB MATERIAL (H).

Figure 13. - Microsection through rubbed node on Hastelloy-X honeycomb. Rub speed was 183 m/sec, the incursion rate was 25.4×10^{-6} m/sec, and the test temperature was 23^{0}C.

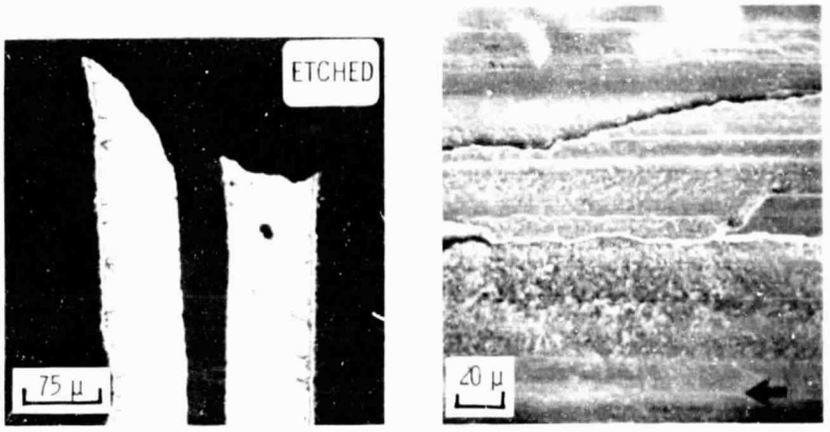

(a) SECTION THROUGH RUBBED NODE.

(b) OVERVIEW OF RUBBED SURFACE.

Figure 14. - Pack aluminide coated honeycomb after 305 m/sec rub at 25.4×10^{-6} m/sec incursion rate, 23^{0} C.

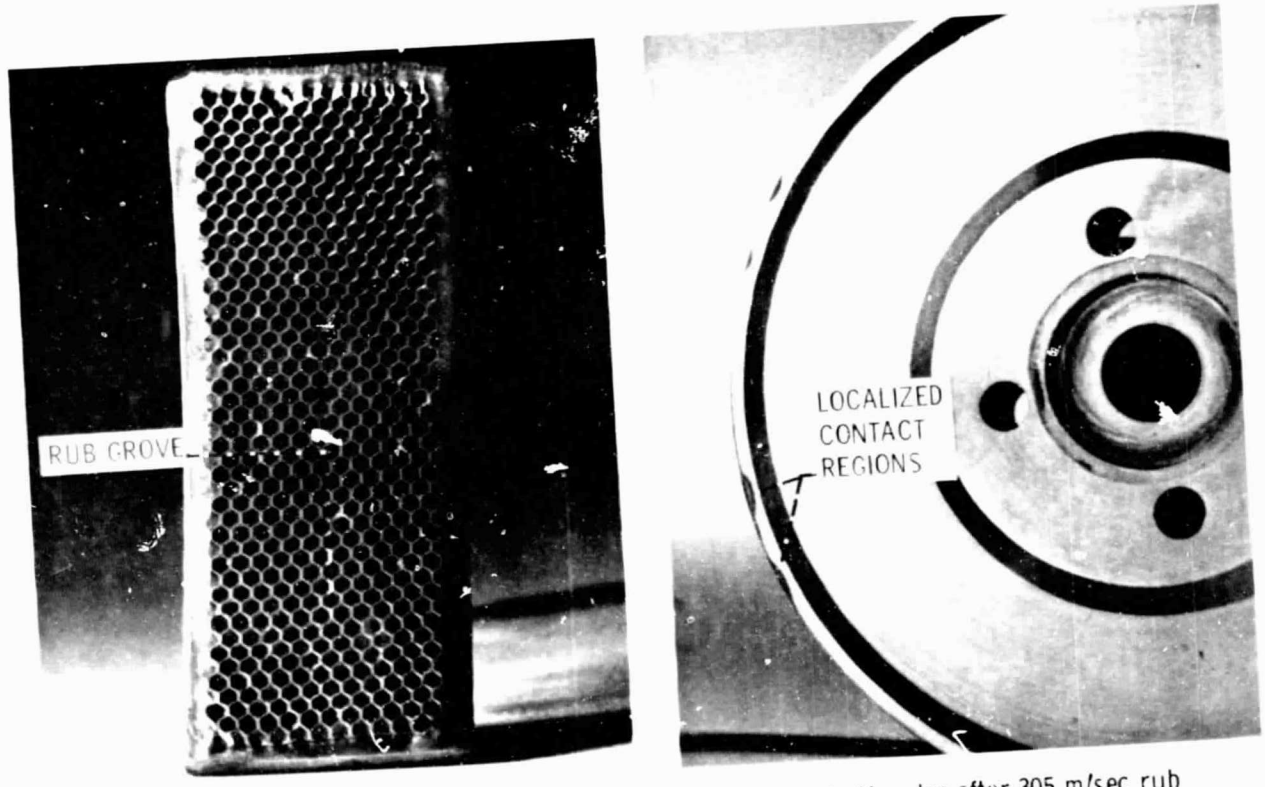

Figure 15. - Pack aluminide coated honeycomb and Waspalloy knife-edge after 305 m/sec rub at 1366^{0} K, 254×10^{-6} m/sec incursion rate.

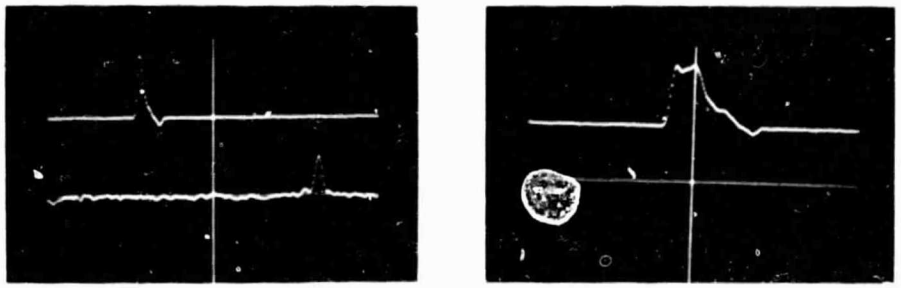

(a) TOP TRACE, ABOUT 20^0 FROM CONTACT. BOTTOM TRACE, 90^0 FROM TOP TRACE.

(b) ENLARGEMENT OF TOP TRACE, INDICATING 1311^0 K MAXIMUM, AND TEMPERATURE, OVER 20^0 ARC.

Figure 16. - High speed pyrometry data from rub interactiom between a Waspalloy knife-edge and Hastelloy-X honeycomb. Rub speed was 305 m/sec, incursion rate was 25.4×10^{-6} m/sec, the test temperature was 23^0 C.

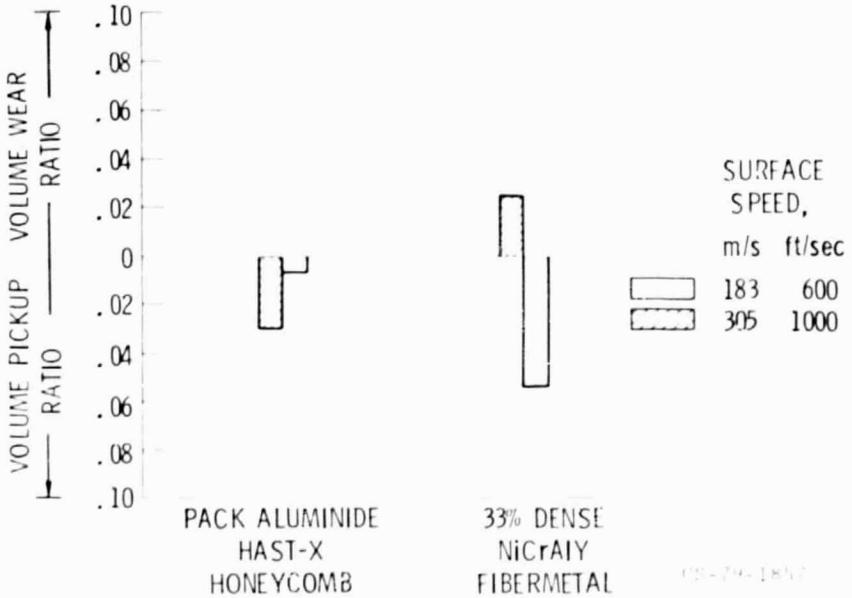

Figure 17. - Volume wear ratio of pack aluminide coated honeycomb and NiCrAlY fiber-metal at 1366^0 K and under 25.4×10^{-6} m/sec incursion rate conditions.

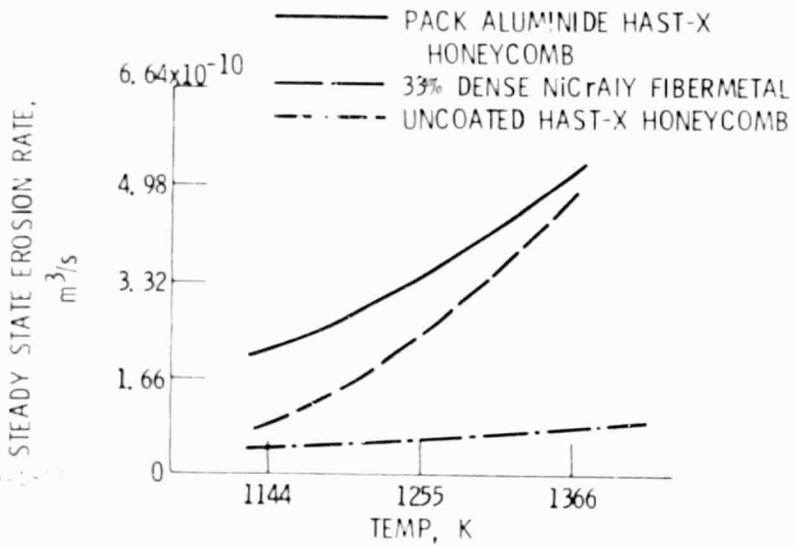

Figure 18. - Volume loss particulate erosion rate versus temperature.

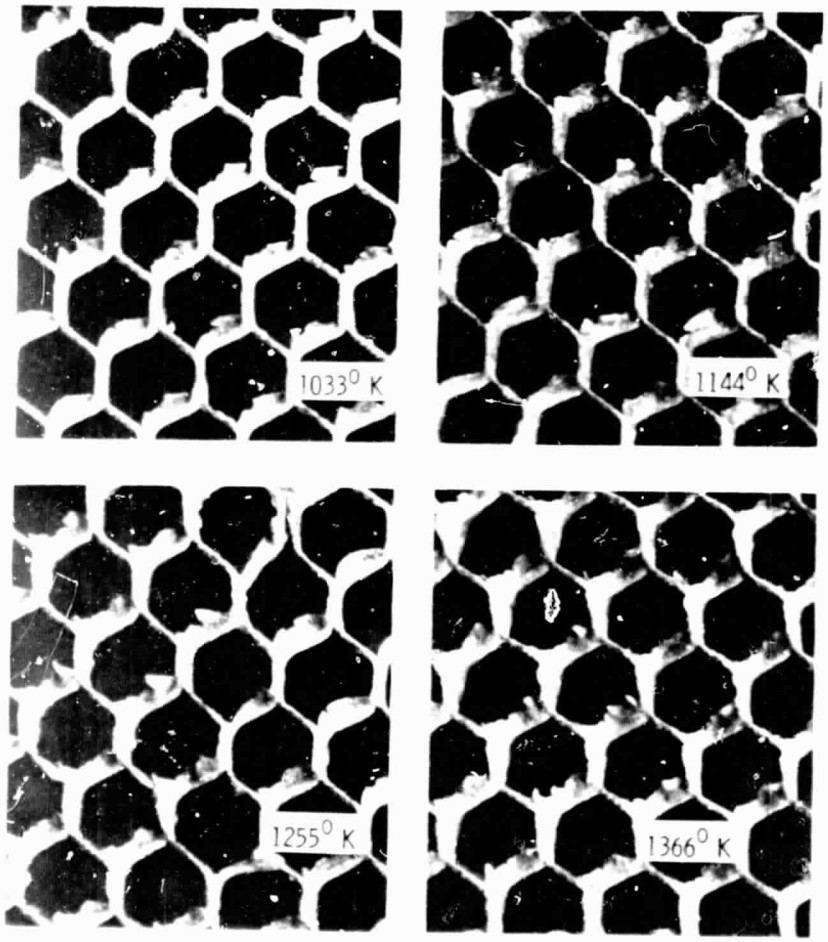

Figure 19. - 1.6 mm cell Hasteiloy-X honeycomb specimens after being subjected to particulate erosion at the indicated temperatures.

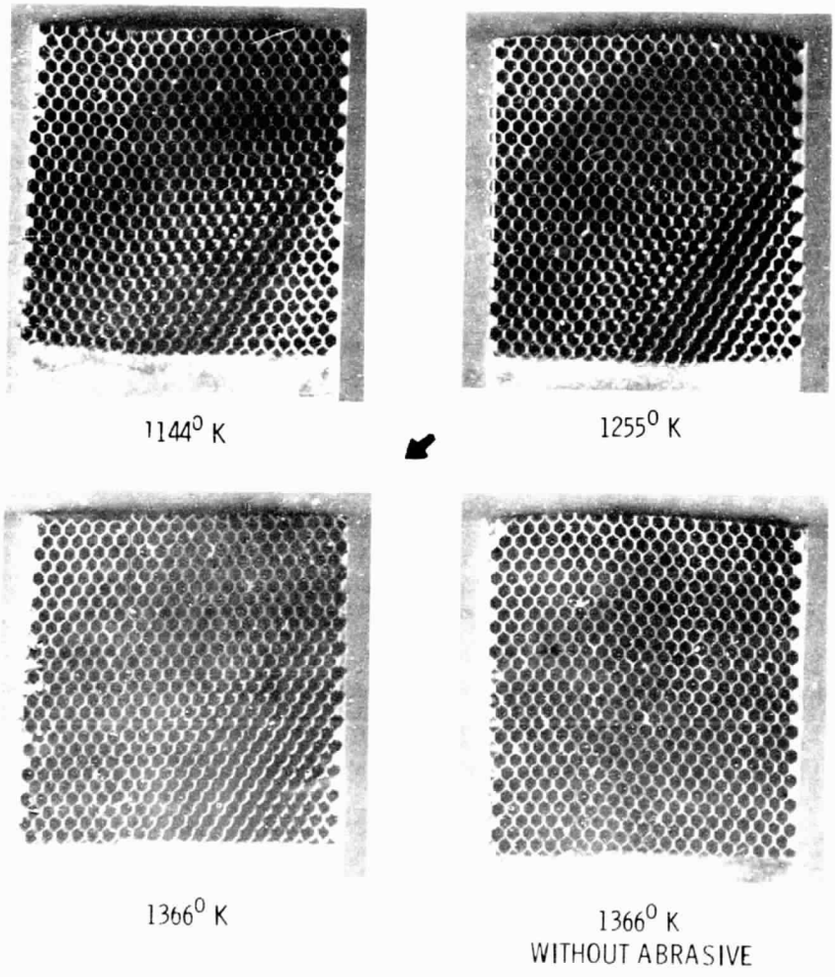

Figure 20. - Pack aluminide coated honeycomb specimens after being subjected to particulate erosion at the indicated temperature.

1. Report No. NASA TM-81398 AVRADCOM TR 79-33	2. Government Accession No.	3. Recipient's Catalog No.
4. Title and Subtitle SOME CONSIDERATIONS OF THE PERFORMANCE OF TWO HONEYCOMB GAS PATH SEAL MATERIAL SYSTEMS		5. Report Date 6. Performing Organization Code
7. Author(s) Robert C. Bill and Lawrence T. Shiembob		8. Performing Organization Report No. E-032
9. Performing Organization Name and Address NASA Lewis Research Center and AVRADCOM Research and Technology Laboratories Cleveland, Ohio 44135		10. Work Unit No. 11. Contract or Grant No.
12. Sponsoring Agency Name and Address National Aeronautics and Space Administration Washington, D.C. 20546 and U.S. Army Aviation Research and Development Command, St. Louis, Mo. 53166		13. Type of Report and Period Covered Technical Memorandum 14. Sponsoring Agency Code

15. Supplementary Notes

Robert C. Bill, Propulsion Laboratory, AVRADCOM Research and Technology Laboratories, Lewis Research Center, Cleveland, Ohio; and Lawrence T. Shiembob, Pratt & Whitney Aircraft Group, East Hartford, Connecticut 06108.

16. Abstract

A standard Hastelloy-X honeycomb material and a pack aluminide coated honeycomb material were evaluated as to their performance as labyrinth seal materials for aircraft gas turbine engines. Consideration from published literature was given to the fluid sealing characteristics of two honeycomb materials in labyrinth seal applications, and their rub characteristics, erosion resistance and oxidation resistance were evaluated. The increased temperature potential of the coated honeycomb material compared to the uncoated standard could be achieved without compromising the honeycomb material's rub tolerance, although there was some penalty in terms of reduced erosion resistance.

17. Key Words (Suggested by Author(s))		18. Distribution Statement
Abradable seal Friction Wear	Erosion Honeycomb	Unclassified - unlimited STAR Category 26

19. Security Classif. (of this report)	20. Security Classif. (of this page)	21. No. of Pages	22. Price*
Unclassified	Unclassified		

* For sale by the National Technical Information Service, Springfield, Virginia 22161